Standardized Direct Charge Device ESD Test For Magnetoresistive Recording Heads I

Tim Cheung (2), Lydia Baril (1), Albert Wallash (1)

(1) Maxtor Corporation, 500 McCarthy Blvd, Milpitas, CA 95035 USA
Tel.: 408-324-7067, fax: 408-894-3207, e-mail: lydia_baril@maxtor.com
(2) Previously at ReadRite Corporation, 44100 Osgood Rd, Fremont, CA 94359 USA
Tel: 805-967-8152, email: tocheung2u@yahoo.com

Abstract – The effects of the Human Body Model (HBM) Electrostatic Discharge (ESD) waveform on Giant Magnetoresistive (GMR) recording heads is well characterized. This information has provided a starting point for understanding ESD damage to magnetic recording heads but the HBM no longer reflect the reality of ESD mechanisms along the production lines. Damage will most likely occur from metal contact to the MR electrodes (metal) rather than from bare fingers. Direct Charged Device Model (DCDM) can be used to simulate metal-to-metal contact discharge. A manual DCDM was characterized using disk capacitors. DCDM manual ESD testing of grounded (suspension is grounded) and floating suspension (suspension is not connected to ground) GMR heads was performed, and a DCDM breakdown voltage ranging from 3V to 9V was measured. Pspice simulation was used to simulate the DCDM discharging events, the results agree well with the DCDM manual discharge data.

I. Introduction

It is well known the GMR heads are sensitive to damage from an electrostatic discharge (ESD) event, as the areal density increases dramatically in magnetic recording industry, the magnetic recording heads become more susceptible to electro-overstress (EOS), and electrostatic discharge (ESD) events. HBM no longer reflects the reality of ESD damage along the manufacturing lines. ESD will mostly occur from direct charging the GMR head capacitances then followed by metal contact to an input, MR+ or MR-, of a GMR head. ESD damage to GMR heads during all stages of handling and assembly is a serious problem in magnetic recording head manufacturing. The GMR sensor will have a voltage if the sensor is itself charged, or if it is in the electric field of a nearby, charged insulator. Tribocharging during handling of a head gimbal assembly (HGA) with an insulating Kapton flex circuit has often been the root cause of severe ESD problems. ESD testing that directly charges and then grounds the MR+ or MR- of a GMR head, known as "DCDM" shows that if the GMR sensor at about 4V is grounded, then the current that flows through the GMR sensor is severe enough to change the sensor resistance. The discharge current waveform from metal contact and DCDM to a GMR head are similar. The purpose of this paper is to characterize the DCDM and understand how the system behaves using disk capacitors, GMR heads, and Pspice simulations.

II. Experimental Setup

The experimental setup consisted of the following components:

1) Manual DCDM test jig
2) Tektronix CT-6 current probe
3) Tektronix 3GHz TDS694C Digital Oscilloscope
4) HP Digital Control Power Supply
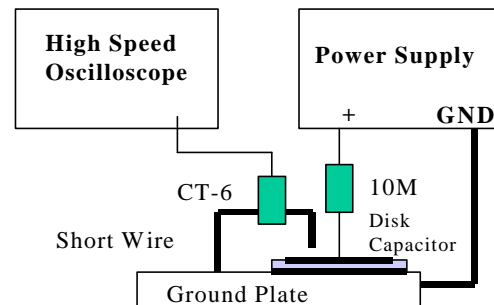5) Gold plated metal plate
6) Disk capacitors

Figure 1a. Schematic representation of the DCDM manual test jig for disk capacitors.

The purpose of using a manual test jig is that it has very small parasitic capacitance and inductance. Figure 1a shows the schematic representation of DCDM manual test jig. The inductanceless disk capacitors are made out of 0.8 mm thick FR-4 double-sided printed circuit board (PCB). One side of the board is gold-plated etched to a circular disk, and the other is gold-plated ground plane. The capacitance depends on the size of a circular disk (the spacing is fixed). The larger the circular disk is the higher the capacitance. Figure 1b shows four different sizes of disk capacitance, 0.5pF, 2.2pF, 4.4pF, and 11.5pF.

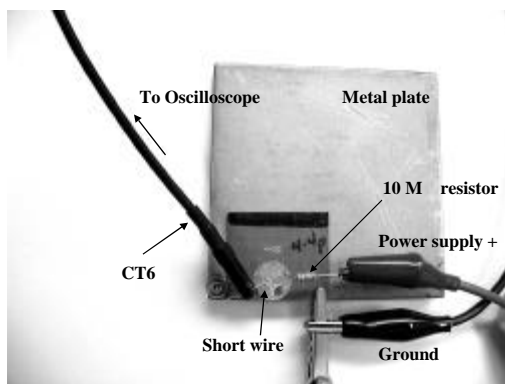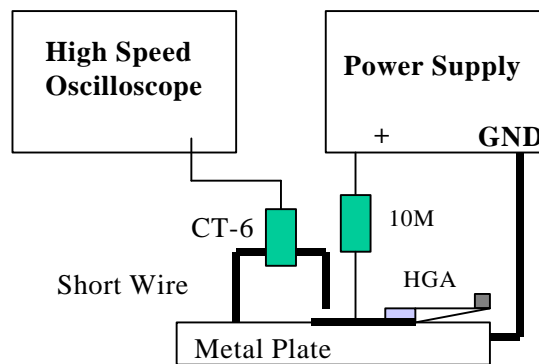Figure 1b. Four disk capacitors 0.5pF, 2.2pF, 4.4pF and 11.5pF.

Figure 1c. DCDM manual test jig for disk capacitors.

The bottom plate of the capacitor lies on a grounded gold-plated metal. The grounded metal plate is gold-plated for good contact between the bottom plate of disk capacitor and metal plate. A voltage source provides voltage to the top plate of the disk capacitor through a 10M resistor. The voltage source is continuously charging the disk capacitor. A short wire of about half inch long is connected to a grounded metal plate through a CT-6 current probe (See Figure 1c). The disk capacitor surface and the grounded wire must be cleaned. The discharge of the disk capacitor is done manually contacting one end of the ground wire to the top disk plate. During discharge process, the manual contact must be very fast and precise. The discharge current waveforms are detected with a CT-6 current probe and the waveforms are captured from a high-speed digital oscilloscope Tektronix TDS 694C 3GHz and 10GS/s.

Figure 2 shows that the grounded and floating suspension GMR heads were tested on the same DCDM manual test jig. A grounded suspension HGA means that the suspension contacts the grounded metal plate. A floating suspension HGA means that the suspension is isolated from the grounded metal plate. A 10M resistor is connected from a power supply to the MR+ of a GMR head. Then, the grounded short wire contacts the MR+ or MR- pad for discharge the charged GMR head. The CT-6 current probe captures the discharge current; the high speed oscilloscope is used to monitor the discharge current, and an Ohmmeter is used to measure the MR resistance after each discharge event until the MR resistance changed more than 1%. (Note: Use the MR resistance failure for reference only, magnetic

performance is more susceptible to ESD damage).

Figure 2. Schematic representation of the DCDM manual test jig for GMR head.

III. Experimental Results and Analysis

Figure 3 shows a simplified electrical equivalent circuit for DCDM manual test jig. The voltage source is not shown in the circuit. C_{disk} is the disk capacitor, L_1 is the inductance of the grounded wire, C_p is the parasitic capacitance of the circuit, R_{spark} is the spark resistance, which is created during the grounded wire contacts the charged disk capacitor.
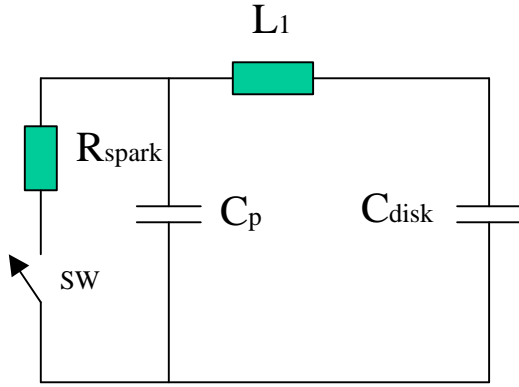
Figure 3. Electrical equivalent circuit for DCDM manual testing for disk capacitor.

Figure 4 shows an example of discharge current waveform for a disk capacitor 4.4pF at charging voltage of 4V. The first peak current reaches 54mA and the pulse width is about 0.47ns. There is a second peak of opposite polarity or undershoot. Its peak current level is about –21mA. Waveforms obtained in the same manner for the same capacitance and the same charging voltage is mostly reproducible, i.e. peak current and pulse width values are within +/- 10%. Waveforms were captured for a range of capacitor values and charging voltages.
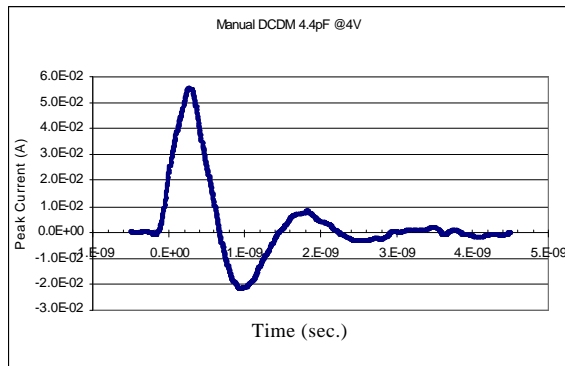

Figure 4. Discharge current waveform of a 4.4pF disk capacitor at 4V.

Figure 5a shows the manual test discharge current for four different capacitances and voltages. The

discharge current equation is given by:

$$I(t) = \frac{V}{\omega L} e^{-\alpha t} \sin(\omega t) \qquad (3)$$

where $\alpha = R/2L$, $\omega = 2\pi f = \sqrt{\frac{1}{LC} - \left(\frac{R}{2L}\right)^2}$,

$I(t)$ is the discharge current and V is the voltage on the capacitor. The equation (3) shows that the voltage on the capacitor is doubled, the discharge current is also doubled. Figure 5b shows that the pulse width decreases as the voltage on the capacitor increases. The hypothesis for the decreasing pulse width at higher voltage are the bandwidth limitation of a CT-6 current probe and the lower spark resistance as a result of smaller change of time constant. Figure 5c shows the discharge current saturated at high capacitance. This is due to the smaller the capacitance, the higher the discharge path impedance, which limits the current. The magnitude of impedance Z is given by:

$$|Z| = \sqrt{R^2 + (\omega L)^2},$$

where $\omega = 2\pi f$, R is the equivalent resistance of the inductor L_1, the L is the inductance of the L_1. Pspice simulation will be used to verify this behavior.
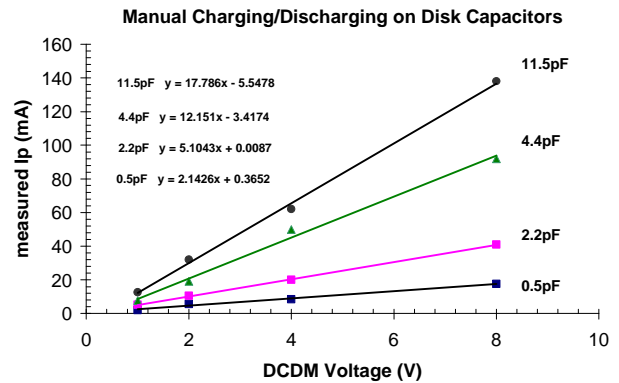

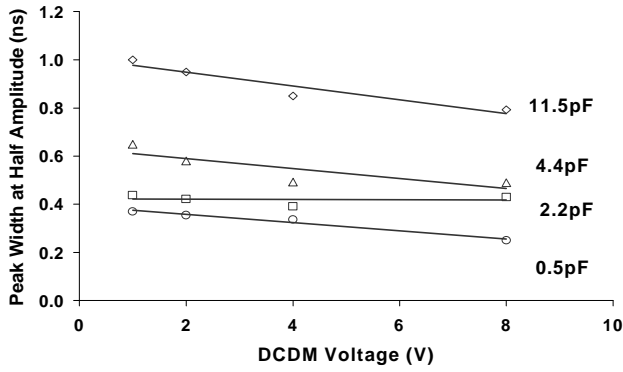Figure 5a. Charging voltage versus discharge current for four capacitors.

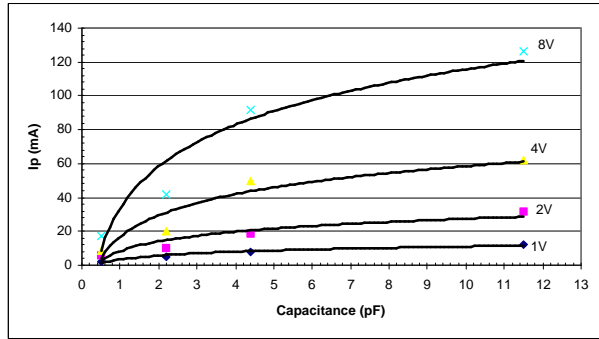Figure 5b. Pulse width versus charging voltage for four capacitances.

Figure 5c. Discharge current versus capacitance for four charging voltages.

Figure 6 shows an electrical circuit model of the DCDM manual testing for grounded suspension GMR heads. The capacitance from the MR leads to suspension is larger than other capacitance when the suspension is grounded. The total capacitance of the HGA depends on the type of flexcircuit. In this particular flexcircuit HGAs, the total capacitance is about 22pF from the MR leads to suspension. Figure 7 shows a simplified equivalent electrical circuit of Figure 6. Where 22pF is the total head capacitance, L_1 is the total inductance of the MR lead and inductance of discharge path.
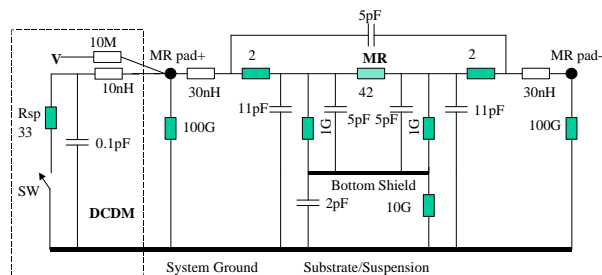

Figure 6. Electrical circuit model of the DCDM manual testing for grounded suspension GMR heads.
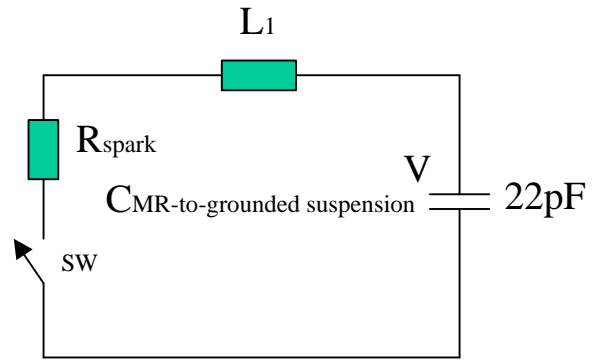

Figure 7. Simplified equivalent electrical circuit model for grounded suspension GMR heads.

Figure 8 shows the discharge current of 51mA and the pulse width of about 2ns at 4V for the grounded suspension GMR head.
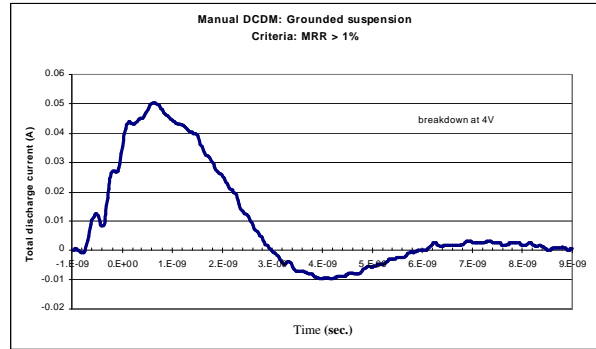

Figure 8. Discharge current waveform at 4V for grounded suspension GMR head.

Figure 9 shows the electrical circuit model of the DCDM, and the floating suspension GMR heads (floating suspension means the suspension is not connected to ground). The head capacitance is dominated by the capacitance between the suspension and the system ground.
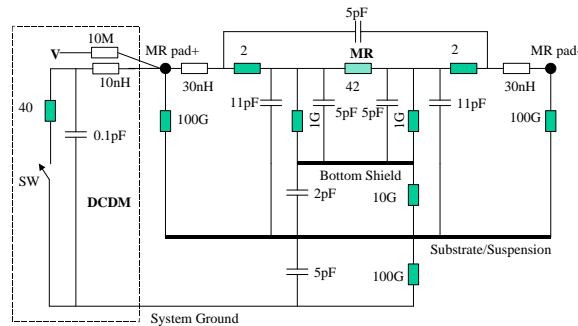

Figure 9. Electrical circuit model of the DCDM and the floating suspension GMR heads.

When the GMR head suspension is not grounded, the capacitance from suspension to grounded metal plate is approximately 5pF. Figure 10a shows the $C_{MR\text{-to-}}$ suspension in series with the $C_{suspension\text{-to-ground}}$. The total head capacitance can be calculated as follows:

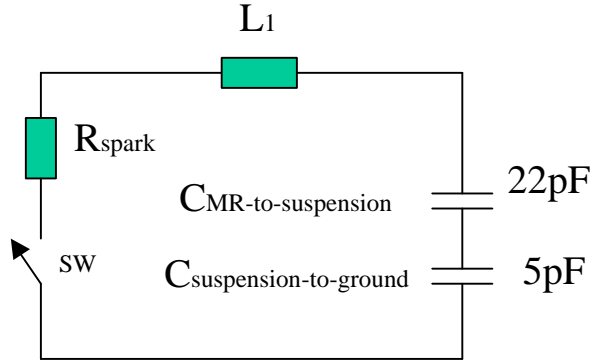$$C=(22pF)(5pF)/(22pF+5pF)=4pF$$

Figure 10a. Simplified electrical circuit model for a floating suspension GMR head.

Figure 10b shows a simplified head capacitance from MR-to-ground for floating suspension GMR head. An equivalent head capacitance can be represented by a single 4pF.
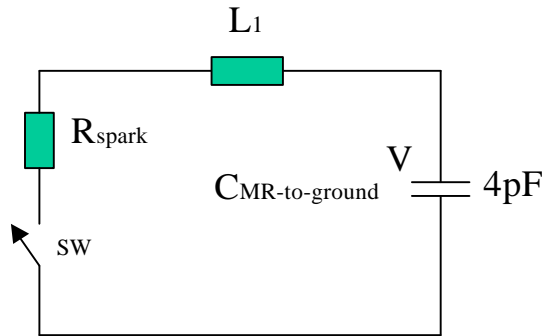

Figure 10b. Simplified electrical circuit model for a floating suspension GMR heads with a total equivalent capacitance of 4pF.

Figure 11 shows the discharge current waveforms at different charging voltages from 3V to 9V. The MR resistance of this floating suspension head changed from 42 to 54 at 9V breakdown. The peak current amplitude at 9V is about 65mA, and the pulse width is about 0.8ns.
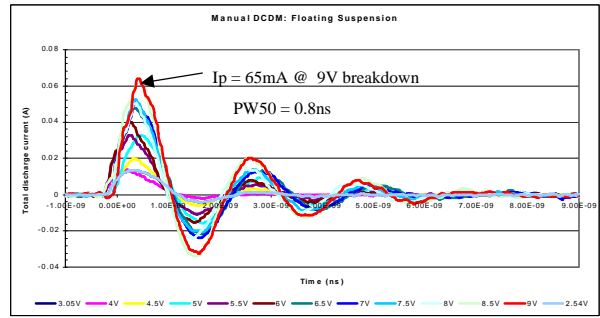

Figure 11. Discharge current waveform at breakdown voltage of 9V for a floating suspension GMR head.

Figure 12 shows that the comparison of the breakdown voltage for the grounded suspension and the floating suspension GMR heads. The grounded suspension heads were broken down at about 3V to 4V, and the floating suspension head was broken down at about 9V at the GMR resistance changing more than 1%. The floating suspension exhibits higher breakdown voltage than the grounded suspension GMR head because the grounded suspension has a larger head capacitance than the floating suspension GMR head reference to grounded metal plate. The grounded suspension HGA has a total head capacitance of about 22pF, and the floating suspension HGA has a total head capacitance of about 4pF. The total head energy to damage to MR sensor can be calculated and compared as follows:

For grounded suspension HGA:
A total head capacitance C of 22pF with a charging voltage (V) at breakdown of 4V, then the total energy can be calculated based on the equation:

$$E=1/2(C\ V^{2})=0.176nJ$$

For floating suspension HGA:
A total equivalent head capacitance C of 4pF with a charging voltage (V) at breakdown of 9V, then the total energy can be calculated based on the equation:

$$E=1/2(C\ V^{2})=0.162nJ$$

Comparing the two total energies, the floating suspension HGA requires higher voltage to reach the same energy level as for the grounded suspension HGA that can damage the GMR sensor (assume same MR resistance for both type). This is due to the floating suspension HGA has lower head capacitance than the grounded suspension HGA reference to ground.
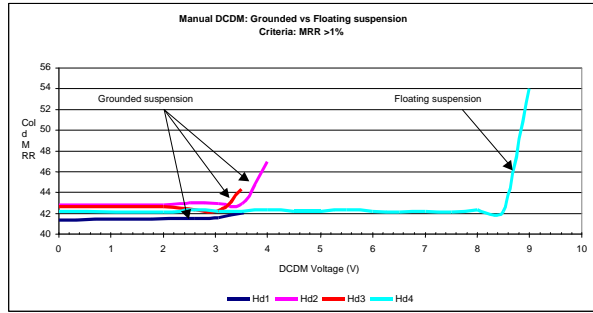
Figure 12. GMR resistance versus DCDM breakdown voltage for grounded and floating suspension GMR heads.

Discharge current occurs when the grounded wire is brought near a charged disk capacitor, the electric field between them increases to an extreme value. When the field exceeds the dielectric breakdown strength of air, current begins to flow by an avalanche process. Eventually a low resistance spark develops. The spark resistance can be affected by the contact conditions such as humidity, contact speed, grounded wire/disk capacitor plate material, the size and the shape of the grounded wire tip and the contamination between the grounded wire tip and the disk capacitor. The following setup can be used for initial spark resistance study.

Figure 13 shows the spark resistance test setup. A low inductance surface mount resistor must be used. The purpose of using additional resistance in series with the discharge path is that the behavior of the pulse width and the amplitude of the discharge current can be observed. (See Figure 14)
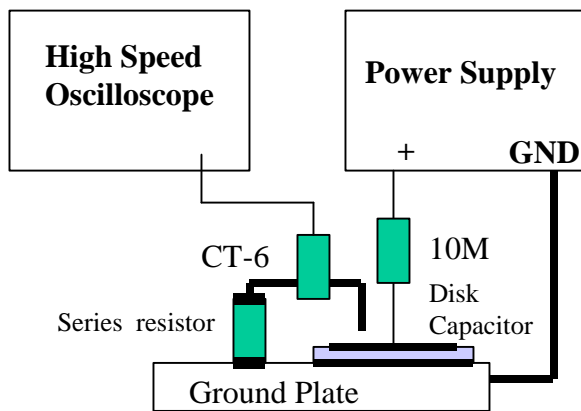

Figure 13. Schematic representation of the spark resistance test setup.

Figure 14 shows the discharge current waveforms varying the different series resistances. The higher the series resistance in the discharge path is the lower the discharge current amplitude and wider the pulse width. Both the resistance and impedance of the inductor L_1 in the discharge path can affect the discharge current amplitude and the pulse wide.

The total resistance, R_t, in the discharge path is approximately related by the following expression:

$$R_t = R_{series} + R_{spark} + |Z| \qquad (4)$$

The magnitude of impedance Z is given by:

$$|Z| = \sqrt{R^2 + (\omega L)^2} \ , \qquad (5)$$

where $\omega = 2\pi f$, R is the equivalent resistance of the inductor wire and L is the equivalent inductance, f is the frequency. The Rspark and the impedance can be calculated from the Equation (4):

$$R_{spark} + |Z| = V_c/I_p - R_{series}$$

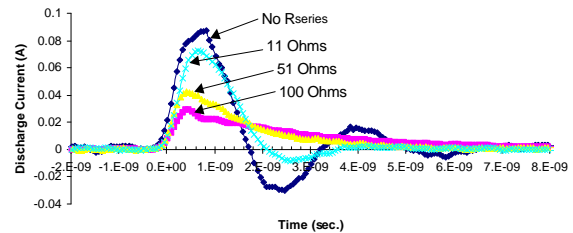where V_c is the charging voltage on the capacitor, and the I_p is the discharging current.

Figure 14. Discharge current versus Rseries at charging voltage of 4V.

Figure 15 shows the Rspark and the impedance Z as a function of charging voltage. The manual DCDM test jig was used to perform this experiment (See Figure 13). The spark resistance plus the impedance Z without adding the series resistance is 44Ω at 4V. Based on the experimental data, the Rspark plus the impedance Z increase as the charging voltage decreases. However, we expected higher spark resistance with the increasing of the charging voltage. More experiments need to be conducted and analyzed in this area.
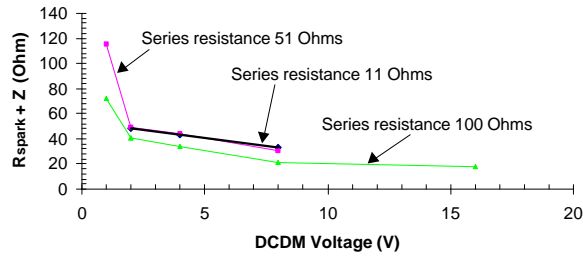
Figure 15. Spark resistance versus DCDM voltage

IV. Pspice Simulation

The DCDM manual discharge behavior can be confirmed by Pspice simulation.

Figure 16 shows the Pspice simulation of discharge current waveform from discharging a disk capacitor of 4.4pF at 4V, inductance L_1 of 10nH and spark resistance of 24 . As can be seen, the DCDM manual discharge waveform and the Pspice simulation waveform are comparable.
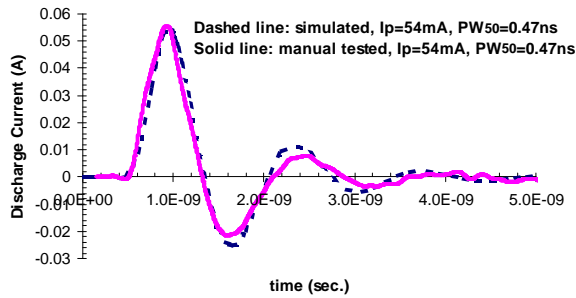

Figure 16. DCDM manual testing (solid line) and simulation (dashed line) comparison using 4.4pF at 4V.
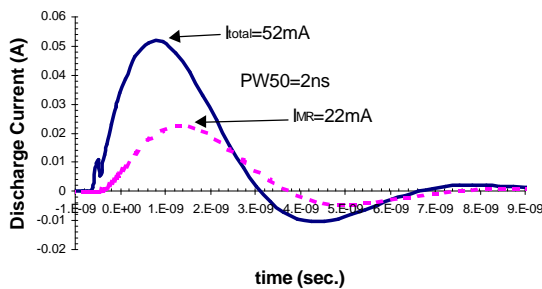

Figure 17. Pspice simulation of discharge current for the grounded suspension GMR head at 4V. Dashed line is the current through GMR sensor.

The total current flows through the GMR heads can be measured but the current flows through the GMR sensor can not be measured. Pspice simulation can be used to observe the current flows through the GMR sensor. Figure 17 shows the Pspice simulation of the total discharge current (solid line), and the current flows through the GMR sensor (dashed line) for the grounded suspension GMR head at breakdown voltage of 4V. The discharge current of 22mA flows through the GMR sensor. The reason for the current flows through the GMR sensor less than 50% of the total current because the GMR sensor resistance limits the current. The total discharge current using the manual discharge (See Figure 8), and the Pspice simulation (See Figure 17) for a grounded suspension GMR head are comparable.

The Pspice simulated discharge current for the floating suspension GMR head at the breakdown voltage of 9V (See Figure 18) is comparable to the manual discharge (See Figure 11). The total discharge current is about 66mA; 22mA flows through the GMR sensor, and the pulse width is about 0.8ns.

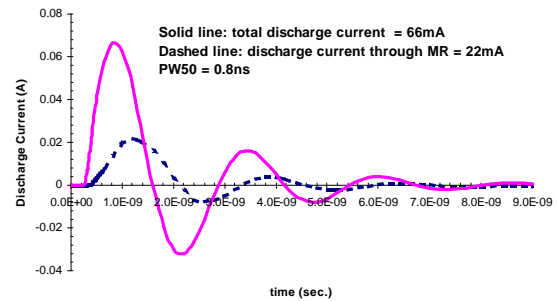Figure 18. Pspice simulation of discharge current for a floating suspension GMR head. Dashed line is the current through GMR sensor.

Figure 19 shows the Pspice simulation of discharge current per charging voltage (mA/V) relationship for 4 different disk capacitors. The simulation results agree well with the DCDM manual discharge.
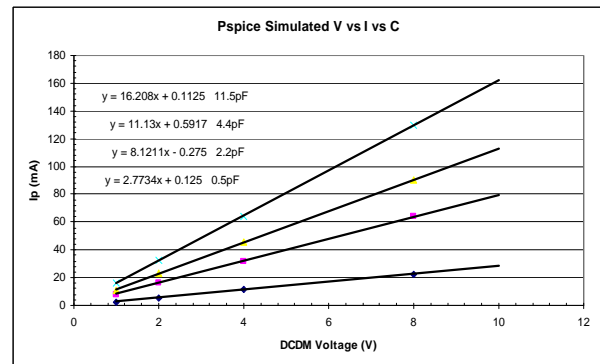

Figure 19. Pspice simulation of peak current versus DCDM voltage.

Figure 20 shows the Pspice simulation of discharge current pulse width as a function of DCDM voltage for 6 different disk capacitors. The spark resistance, inductance and capacitance are no changed. The pulse width maintains constant throughout the charging voltage ranging from 1V to 16V. However, the simulation conditions and the experimental condition is slightly different. The experimental data shows that the spark resistance changes as varying the charging voltage.
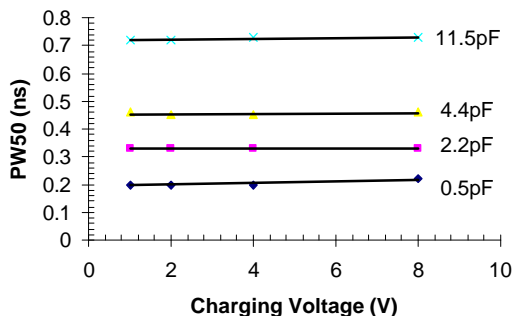

Figure 20. Pspice simulation of discharge current pulse width versus charging voltage.

Figure 21 shows the discharge currents are saturated as increasing the capacitance. The experimental data and simulation data are comparable.
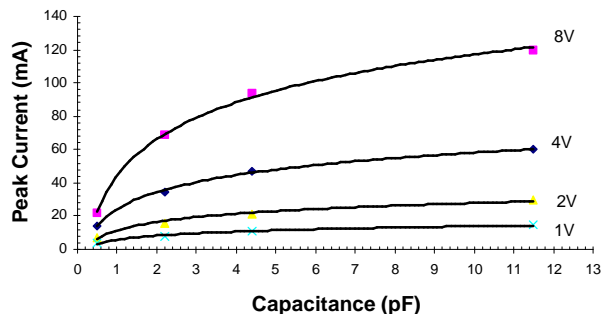

Figure 21. Pspice simulation of discharge current versus capacitance for four charging voltages.

Figure 22 shows that if the DCDM module varies the spark resistance from 10   to 60   during ESD testing, 75% less energy (not shown) flows through the GMR sensor at 60? .
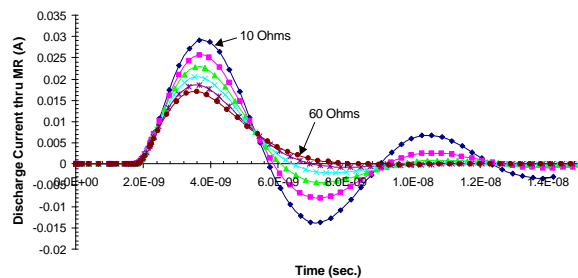

Figure 22. Pspice simulation of discharge current flows through the GMR sensor at the charging voltage of 4V with varying the spark resistance Rsp of the DCDM from 10   to 60   .

Figure 23 shows that if the DCDM module varies the discharge path inductance from 5nH to 65nH, the energy (not shown) increases about 23% at 65nH.
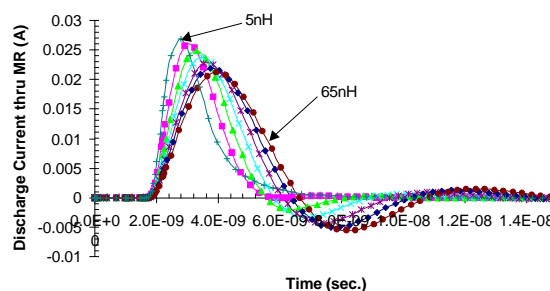

Figure 23. Pspice simulation of discharge current flows through the GMR sensor at the charging voltage of 4V with varying the discharge path inductance from 5 to 65nH.

V. Data Summary

Table 1 shows the rise time of discharge currents for four capacitors at charging voltage ranging from 1V, 2V, 4V and 8V.   The experimental (exp) and simulation (sim) results are closed.

tr (ns)	0.5pF		2.2pF		4.4pF		11.5pF	
	exp	sim	exp	sim	exp	sim	exp	sim
V								
1	0.25	0.177	0.21	0.203	0.39	0.215	0.53	0.32
2	0.18	0.17	0.25	0.197	0.31	0.226	0.42	0.32
4	0.17	0.175	0.26	0.209	0.29	0.225	0.4	0.32
8	0.14	0.175	0.19	0.192	0.34	0.228	0.44	0.32
Ave	0.19	0.17	0.23	0.20	0.33	0.22	0.45	0.32

Table 1. Discharge current risetime comparison for four capacitances at charging voltages ranging from 1V, 2V, 4V and 8V.

Table 2 shows the sensitivity of discharge current per charging voltage (mA/V) for four capacitances. There is about 9% different between experimental and simulation results for both 11.5pF and 4.4pF.

	0.5pF		2.2pF		4.4pF		11.5pF	
	exp	sim	exp	sim	exp	sim	exp	sim
mA/V	2.14	2.8	5.1	8.1	12.2	11.1	17.8	16.2

Table 2. Discharge current per charging voltage sensitivity comparison for four capacitances.

Table 3 shows the pulse width for four capacitances at charging voltage ranging from 1V, 2V, 4V and 8V. The experimental and simulation results are close, but the simulation data are slightly less than the experimental data. Selection of component values for simulation can affect the results.

PW50	0.5pF		2.2pF		4.4pF		11.5pF	
	exp	sim	exp	sim	exp	sim	exp	sim
V								
1	0.37	0.2	0.44	0.33	0.65	0.46	1.00	0.72
2	0.35	0.2	0.42	0.33	0.58	0.45	0.95	0.72
4	0.34	0.2	0.39	0.33	0.49	0.45	0.85	0.73
8	0.25	0.22	0.43	0.33	0.49	0.46	0.79	0.73
Ave	0.33	0.21	0.42	0.33	0.55	0.46	0.90	0.73

Table 3. Discharge current pulse width comparison for four capacitances at charging voltages ranging from 1V, 2V, 4V and 8V.

VI. Conclusion

We have learned from the manual testing, and Pspice simulations, the spark resistance; parasitic capacitance and inductance of the DCDM system can change the characteristic of a DCDM discharging current waveform. The Pspice simulation and experimental data are comparable. The data shows the grounded suspension GMR head is more sensitive than the floating suspension GMR head. The spark resistance, the DCDM parasitic inductance and capacitance can affect the results of ESD testing. More spark resistance experiments need to be conducted and analyzed. It is a big challenge for the test equipment vendors to design a DCDM tester with very small parasitic inductance and capacitance.

REFERENCES

[1] Socket Device Model Testing, ESD Association technical report TR 08-00
[2] The SDM Test Method: Past, Present, and Future. Michael Chaine, Ion Barth, Tilo Bordeck, Leo G. Henry, Mark A. Kelly, and Tom Meusen Compliance Engineering. Ce-mag.com 09-10/2001
[3] Charge Device Model. ESD Association standard test method. ESD STM5.3.1-1999
[4] Standardized Direct Charged Device ESD Test for Magnetoresistive Recording Heads II. Lydia Baril, Tim Cheung, Albert Wallash. Submitted to EOS/ESD Symposium 2002
[5] "Direct Charging" Charge Device Model Testing of Magnetoresistive Recording Heads. Tim Cheung, EOS/ESD Symposium 1997